J. Chem. Eng. Data **2011,** *56,* 185–189

Solid−Liquid Equilibrium and Activity Coefficients for Binary Mixtures of Caprolactam and Cyclohexanone Oxime with Room-Temperature Ionic Liquids

Marina P. Shevelyova,* Yauheni U. Paulechka, Gennady J. Kabo, and Anton S. Halauko

Chemistry Faculty and Research Institute for Physical Chemical Problems, Belarusian State University, Leningradskaya 14, Minsk 220030, Belarus

Solid−liquid equilibria in a wide range of concentrations for binary mixtures of ε-caprolactam (CL) and cyclohexanone oxime (CHO) with 1-butyl-3-methylimidazolium hexafluorophosphate ([C$_4$MIM][PF$_6$]), 1-butyl-3-methylimidazoium tetrafluoroborate ([C$_4$MIM][BF$_4$]), and 1-methyl-3-tetradecylimidazolium bis(trifluoromethanesulfonyl)imide ([C$_{14}$MIM][NTf$_2$]) and CHO with 1-butyl-3-methylimidazolium tosylate ([C$_4$MIM][Tos]) have been studied in this work. Activity coefficients of the components in the saturated solutions were evaluated. Solution enthalpies of the solutes were determined. Solubilities and activity coefficients of CL and CHO in their solutions with 1,3-dialkylimidazolium ionic liquids were compared.

Introduction

Ionic liquids (ILs) have been attracting a large interest as environmentally friendly media for industrially important reactions.[1] Since the Beckmann rearrangement of cyclohexanone oxime (CHO) into caprolactam (CL) carried out during caprolactam production requires relatively a high temperature (400 K) and large amount of oleum (about 1.4 kg per 1 kg of CHO),[2] a search of new media and/or catalysts for the reaction for carrying out the rearrangement at mild conditions and with a renewed catalyst seems to be important. ILs have proved their potential for this process as nonhazardous reaction media with low vapor pressure which allow carrying out the rearrangement at $T < 373$ K.[1,3−5] The liquid-phase Beckmann rearrangement in IL media at ambient temperatures with a high yield and selectivity was reported in ref 3. Gui et al. performed the rearrangement in a task-specific IL as a catalyst and solvent.[4] Verevkin et al.[5] carried out the rearrangement in a solvent with a task-specific IL as a catalyst.

The solid−liquid equilibrium (SLE) diagrams for CHO and CL with ILs would promote the correct choice of conditions for the Beckmann rearrangement and the subsequent product separation. The activity coefficients and dissolution enthalpies as well as the regularities in these parameters and mutual solubilities can be evaluated using the SLE data.

In this work, SLE for binary mixtures of CL and CHO with 1-butyl-3-methylimidazolium hexafluorophosphate [C$_4$MIM][PF$_6$], 1-butyl-3-methylimidazolium tetrafluoroborate [C$_4$MIM][BF$_4$], 1-butyl-3-methylimidazolium tosylate [C$_4$MIM][Tos], and 1-methyl-3-tetradecylimidazolium bis(trifluoromethanesulfonyl)imide [C$_{14}$MIM][NTf$_2$] was studied. These systems were chosen because of the following reasons. The Beckmann rearrangement was successfully carried out in [C$_4$MIM][PF$_6$] and [C$_4$MIM][BF$_4$],[3] so it seemed reasonable to study SLE for the binaries with those ILs. The parameters of fusion for [C$_4$MIM][Tos] as well as the SLE data for [C$_4$MIM][Tos] + H$_2$O and [C$_4$MIM][Tos] + CL were obtained earlier.[6] The SLE for [C$_4$MIM][Tos] + CHO would complete those data. The SLE data for CL + [C$_{14}$MIM][NTf$_2$] and CHO + [C$_{14}$MIM][NTf$_2$] together with the literature data for similar systems with [C$_6$MIM][NTf$_2$][7] would allow us to analyze the dependence of the solubilities on the alkyl chain length in imidazolium ILs.

Table 1. Purity of the Studied Substances

substance		x_1	ref
1-butyl-3-methylimidazolium hexafluorophosphate	[C$_4$MIM][PF$_6$]	0.995	8
1-butyl-3-methylimidazolium tosylate	[C$_4$MIM][Tos]	0.96	6
1-methyl-3-tetradecylimidazolium bis(trifluoromethanesulfonyl)imide	[C$_{14}$MIM][NTf$_2$]	0.986	9
cyclohexanone oxime	CHO	0.9998	10
caprolactam	CL	0.9998	7

Experimental Section

Materials. The samples of [C$_4$MIM][PF$_6$] (Covalent Associates) and [C$_4$MIM][BF$_4$] (Solvent Innovation) with the initial mass-fraction purity of 0.99 were used. The samples were exposed to a vacuum of 0.1 Pa at $T = 310$ K during 10 h to remove volatile impurities. The sample of [C$_4$MIM][Tos] (Iolitec) was purified by vacuum pumping at 10^{-3} Pa during 30 h at T rising from (323 to 353) K. The sample of [C$_{14}$MIM][NTf$_2$] provided by Prof. Ya. S. Vygodskii was exposed to a vacuum of 10^{-3} Pa during 48 h at T rising from (290 to 373) K. The samples of CHO and CL (Grodno-Azot) with the initial mass-fraction purity of ≥ 0.95 and ≥ 0.995, respectively, were sublimed at $p = 0.3$ kPa and $T = 320$ K. The mole-fraction purity of all of the samples except for [C$_4$MIM][BF$_4$] (Table 1) was determined by the fractional melting technique in an adiabatic calorimeter[6−10] according to the procedure described in ref 11.

SLE by the Visual Method. The mixtures of known compositions were placed in glass tubes of $4 \cdot 10^{-6}$ m^3 volume and $6 \cdot 10^{-3}$ m diameter in a drybox and then hermetically sealed. The uncertainty of weighing was $\pm\ 5 \cdot 10^{-8}$ kg, and the uncertainty in mole fraction caused by the weighing was $\pm\ 1 \cdot 10^{-3}$.

The equilibrium crystalline phases were obtained in the following way. Before each series of experiments the tubes were

---

* To whom the correspondence should be addressed. Tel.: +375-17-2224305. E-mail: shevelyova.marina@yahoo.com.

10.1021/je1005054

Table 2. Parameters of Fusion of the Substances

	T_{tp}	$\Delta_{\mathrm{cr}}^{\mathrm{l}}H_{\mathrm{m}}^{\mathrm{o}}$	$\Delta_{\mathrm{cr}}^{\mathrm{l}}C_{p}^{\mathrm{o}}$	
substance	K	$\mathrm{kJ \cdot mol^{-1}}$	$\mathrm{J \cdot K^{-1} \cdot mol^{-1}}$	ref
$[C_4MIM][PF_6]$	283.51 ± 0.01	19.60 ± 0.02	45 ± 2	8
$[C_4MIM][Tos]$	343.89 ± 0.09	22.8 ± 0.5	34 ± 1	6
$[C_{14}MIM][NTf_2]$	308.72 ± 0.04	45.3 ± 0.4	43 ± 3	9
CHO	362.20 ± 0.04	12.45 ± 0.20	49 ± 1	10
CL	342.22 ± 0.01	16.16 ± 0.02	54 ± 1	7

kept at (340 to 370) K until the components were melted completely, and the content was mixed thoroughly. The obtained uniform solutions were then kept at 243 K for 24 h for crystallization of the components. The content was remelted at slow heating to the temperature close to T^{SLE}, when only a few crystals remained in the mixture. Then, the tube was cooled at a rate of $2 \cdot 10^{-3}\ \mathrm{K \cdot s^{-1}}$ to $T = 273$ K.

A water thermostat was used for the experiments. The temperature was measured with a Hg thermometer with the uncertainty of ± 0.1 K. The liquidus points T^{SLE} were determined at a heating rate of $1 \cdot 10^{-4}\ \mathrm{K \cdot s^{-1}}$ and constant mixing. They were supposed to be the temperatures at which the last crystal disappeared. The liquid−gas volume ratio in the tubes was ∼1:1, and the change of compositions caused by vaporization of the components into the free volume of the tubes was neglected. The uncertainty of T^{SLE} was ± 0.5 K. The method was checked in the experiments with water + cyclohexanone.[7]

Mutual solubilities in the studied systems were calculated by the well-known equation:[12]

$$x_i(T^{\mathrm{SLE}}) = \exp\left(A\left[\frac{1}{T_{\mathrm{tp}}} - \frac{1}{T^{\mathrm{SLE}}}\right] + B\left[\frac{T_{\mathrm{tp}}}{T^{\mathrm{SLE}}} - 1 - \ln\left(\frac{T_{\mathrm{tp}}}{T^{\mathrm{SLE}}}\right)\right]\right) \quad (1)$$

where T_{tp} is the triple point of component i. If the solute is solid-insoluble and the solution is the ideal one, then the parameters of eq 1 mean: $A = \Delta_{\mathrm{cr}}^{\mathrm{l}}H_{\mathrm{m},i}^{\mathrm{o}}(T_{\mathrm{tp}})/R$; $B = \Delta_{\mathrm{cr}}^{\mathrm{l}}C_{p,i}^{\mathrm{o}}(T_{\mathrm{tp}})/R$. The values of T_{tp}, $\Delta_{\mathrm{cr}}^{\mathrm{l}}H_{\mathrm{m},i}^{\mathrm{o}}(T_{\mathrm{tp}})$, and $\Delta_{\mathrm{cr}}^{\mathrm{l}}C_{p,i}^{\mathrm{o}}(T_{\mathrm{tp}})$ for pure CL, CHO, $[C_4MIM][PF_6]$, $[C_4MIM][Tos]$, and $[C_{14}MIM][NTf_2]$ were determined earlier[6−10] (Table 2). In case of the nonideal solution, $A = \Delta_{\mathrm{cr}}^{\mathrm{sol}}H_{\mathrm{m}}^{\mathrm{SLE}}(T_{\mathrm{tp}})/R$; $B = \Delta_{\mathrm{cr}}^{\mathrm{sol}}C_{p,\mathrm{m}}^{\mathrm{SLE}}(T_{\mathrm{tp}})/R$; $\Delta_{\mathrm{cr}}^{\mathrm{sol}}H_{\mathrm{m},i}^{\mathrm{SLE}}$, and $\Delta_{\mathrm{cr}}^{\mathrm{sol}}C_{p,\mathrm{m}\,i}^{\mathrm{SLE}}$ are the enthalpy and the heat capacity changes when going from crystal to the saturated solution containing 1 mol of component i at T_{tp}. The activity coefficients γ_i^{SLE} were calculated as:

$$\gamma_i = \frac{x_i^{\mathrm{id}}(T^{\mathrm{SLE}})}{x_i(T^{\mathrm{SLE}})} \quad (2)$$

where $x_i^{\mathrm{id}}(T^{\mathrm{SLE}})$ is the solubility of component i calculated by eq 1 under the assumption $\gamma_i^{\mathrm{SLE}} = 1$ and $x_i(T^{\mathrm{SLE}})$ is the real solubility of i.

The partial molar excess enthalpies $\bar{H}_{\mathrm{m},i}^{\mathrm{ex}}(T_{\mathrm{tp}})$ were calculated as:

$$\bar{H}_{\mathrm{m},i}^{\mathrm{ex}}(T_{\mathrm{tp}}) = \Delta_{\mathrm{cr}}^{\mathrm{sol}}H_{\mathrm{m},i}^{\mathrm{SLE}}(T_{\mathrm{tp}}) - \Delta_{\mathrm{cr}}^{\mathrm{l}}H_{\mathrm{m},i}^{\mathrm{o}}(T_{\mathrm{tp}}) \quad (3)$$

Quantum-Chemical Calculations. Quantum-chemical calculations were performed using the Firefly QC package,[13] which is partially based on the GAMESS (U.S.)[14] source code. The dipole moments and polarizabilities of the most stable conformers of the CL and CHO molecules as well as the $[C_4mim]BF_4$,

Table 3. SLE Temperatures T^{SLE}, Mole Fractions x^{SLE}, and Activity Coefficients γ^{SLE} of the Solute in the Studied Systems

x_1^{SLE}	$T^{\mathrm{SLE}a}$/K	$\gamma_1^{\mathrm{SLE}b}$	$\gamma_2^{\mathrm{SLE}b}$
CL (1) + $[C_4MIM][PF_6]$ (2)			
1.00	342.22[c]	1.00	
0.870	335.9	1.04	
0.825	333.5	1.05	
0.696	325.7	1.09	
0.578	317.9	1.15	
0.529	314.7	1.18	
0.426	307.5	1.29	
0.336	300.6	1.44	
0.320	306.1		
0.271	298.0		
0.200	278.7		1.09
0.118	280.1		1.03
0.00	283.51[c]		1.00
CL (1) + $[C_4MIM][BF_4]$ (2)			
1.00	342.22[c]	1.00	
0.832	334.6	1.07	
0.770	331.5	1.09	
0.688	325.8	1.09	
0.616	323.3		
0.575	323.0		
0.493	319.2		
0.433	311.8		
0.364	305.2		
0.301	302.7		
0.256	296.1		
0.206	292.2		
CL (1) + $[C_{14}MIM][NTf_2]$ (2)			
1.00	342.22[c]	1.00	
0.934	336.8	0.98	
0.856	328.0	0.92	
0.773	317.2	0.84	
0.661	303.0	0.76	
0.587	293.8	0.72	
0.532	300.9		
0.452	302.1		
0.312	304.5		1.13
0.216	307.4		1.16
0.00	308.72[c]		1.00
CHO (1) + $[C_{14}MIM][NTf_2]$ (2)			
1.00	362.20[c]	1.00	
0.912	361.2	1.08	
0.889	360.9	1.10	
0.736	355.4	1.26	
0.592	349.5	1.47	
0.499	343.0	1.60	
0.408	330.1	1.72	
0.313	312.8	1.79	
0.208	306.8		1.13
0.114	308.1		1.09
0	308.72[c]		1.00
CHO (1) + $[C_4MIM][Tos]$ (2)			
1.00	362.20[c]	1.00	
0.952	359.8	1.02	
0.938	356.9	1.01	
0.924	356.6	1.02	
0.907	354.6		
0.902	355.7		
0.887	355.6		
0.868	355.6		
0.841	354.4		
0.820	354.5		
0.768	353.2		
0.742	349.4		
0.732	349.6		
0.700	344.4		
0.669	351.7		
0.663	348.5		
0.663	347.9		
0.574	328.2		
0.557	322.8		
0.507	310.7		
0.497	305.2		
0.453	312.1		
0.432	314.6		
0.279	329.1		0.99
0.067	341.7		1.02
0.00	343.89[c]		1.00

[a] Saturation temperature. [b] γ_i^{SLE}(exp) calculated with eq 2. [c] Triple-point temperature of the pure solute.

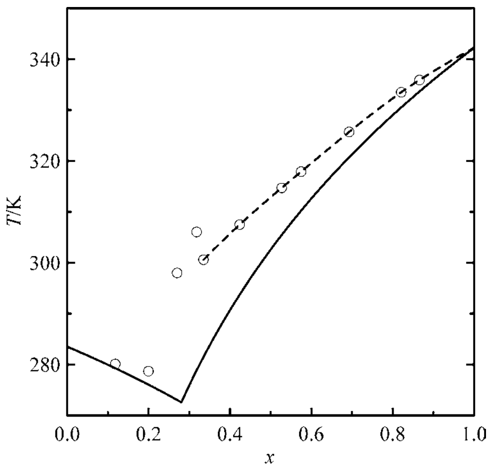

Figure 1. SLE for CL + [C_4MIM][PF_6]. *x*, mole fraction of CL; ○, experimental points; —, ideal solubility curves, - - -, fitting curve (eq 1).

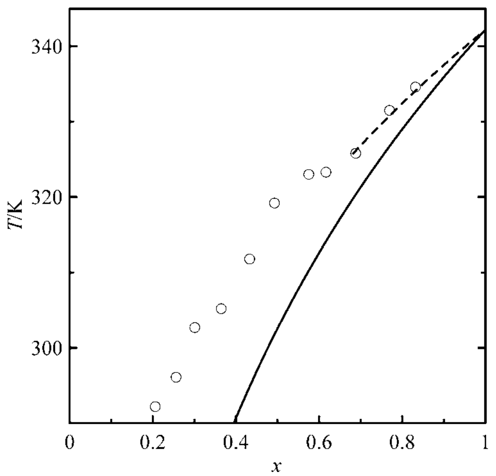

Figure 2. SLE for CL + [C_4MIM][BF_4]. *x*, mole fraction of CL; ○, experimental points; —, ideal solubility curve, - - -, fitting curve (eq 1).

[C_4mim]PF_6, and [C_6mim]NTf_2 ionic pairs were calculated for the geometries optimized in terms of density functional theory (DFT) at the B3LYP/6-311G* theory level.

Results and Discussion

Solid−Liquid Equilibria. The experimental T^{SLE} and the activity coefficients are listed in Table 3, and the phase diagrams are shown in Figures 1 to 4. The experimental values of x^{SLE} and T^{SLE} were fitted with eq 1, and the parameters *A* and *B* of the equation as well as the thermodynamic parameters for the saturated solutions are listed in Table 4.

The solubility of CL in [C_4MIM][PF_6] and [C_4MIM][BF_4] is lower than the ideal one. There is a maximum in the SLE curve for CL + [C_4MIM][PF_6] near CL:[C_4MIM][PF_6] = 1:2, corresponding to an intermolecular compound (Figure 1). The compound melts without decomposition and forms eutectics both with CL and [C_4MIM][PF_6]. The crystalline [C_4MIM][BF_4] have not been reported yet. We also failed to obtain the crystals of [C_4MIM][BF_4] in the CL + [C_4MIM][BF_4] mixture. The components form an intermolecular compound near CL:[C_4MIM][BF_4] = 0.55:0.45, which melts without decomposition (Figure 2). The compound forms a eutectic with CL.

The solubility of CL in [C_{14}MIM][NTf_2] at $T > 307$ K is higher than the ideal one (Figure 3) and close to the solubility of CL in [C_6MIM][NTf_2].[7] The $\Delta_{cr}^{sol}H_m(T_{tp})$ and $\bar{H}_m^{ex}(T_{tp})$ values for CL in CL + [C_{14}MIM][NTf_2] are very close to those for CL in CL + [C_6MIM][NTf_2] (Table 4).

The mutual insolubility of [C_4MIM][PF_6] and [C_4MIM][BF_4] with CHO was established for the mole fractions *x*(CHO) = 0.1 to 0.9 and the temperature interval $T = (290$ to $370)$ K. At $T > T_{tp}$ (CHO) two mutually insoluble liquids were observed. The solubility of CHO in [C_{14}MIM][NTf_2] is significantly lower than the ideal one (Figure 4) and is close to that in [C_6mim]NTf_2.[7]

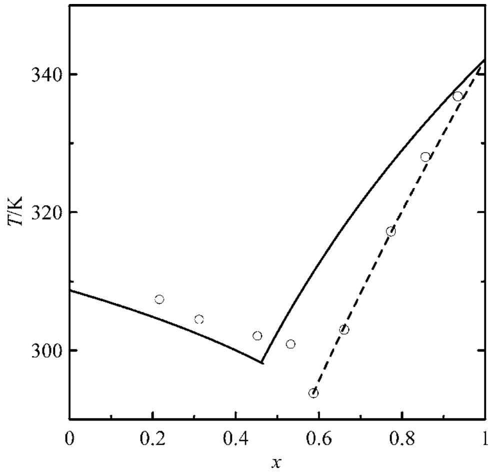

Figure 3. SLE for CL + [C_{14}MIM][NTf_2]; *x*, mole fraction of CL; ○, experimental points; —, ideal solubility curves, - - -, fitting curve (eq 1).

A maximum in the $x_i = f(T^{SLE})$ dependence for CHO + [C_4MIM][Tos] indicates the formation of the intermolecular compound CHO:[C_4MIM][Tos] = 2:1 (($(CHO)_2$[C_4MIM][Tos])), which melts without decomposition (Figure 5) and forms a eutectic with [C_4MIM][Tos] at $T < 305$ K. Over the interval *x*(CHO) = 0.92 to 1.0 the solubility of CHO in [C_4MIM][Tos] is close to the ideal one. At *x*(CHO) = 0.92 ± 0.05 and temperature (355 ± 2) K, a break in the $x(CHO) = f(T^{SLE})$ curve is observed, which proves the formation of one more intermolecular compound of CHO and [C_4MIM][Tos] of unknown composition. The compound forms a eutectic with $(CHO)_2$[C_4MIM][Tos] near *x*(CHO) = 0.70.

Comparison of Solubilities of CL and CHO in ILs. The solubilities of CL and CHO in ILs obtained in this work and available from literature[6,7] are compared in Figure 6. The mole

Table 4. Thermodynamic Parameters of the Components in the Solutions Calculated with Equation 1

system	x_1	$A \cdot 10^{-3}$ / K	*B*	$\Delta_{cr}^{sol}H_m(T_{tp})$ / $kJ \cdot mol^{-1}$	$\bar{H}_{m,1}^{ex}(T_{tp})^a$ / $kJ \cdot mol^{-1}$	$\Delta_{cr}^{sol}C_{p,m1}(T_{tp})$ / $J \cdot K \cdot mol^{-1}$
CL(1)/[C_4MIM][PF_6](2)	0.34−1	2.3 ± 0.1	−18 ± 8	19 ± 1	3 ± 1	−150 ± 60
CL(1)/[C_4MIM][BF_4](2)	0.69−1	2.6 ± 0.1	0^b	22 ± 1	6 ± 1	0
CL(1)/[C_{14}MIM][NTf_2](2)	0.59−1	1.1 ± 0.3	0^b	9 ± 2	−7 ± 2	0
CHO(1)/[C_4MIM][Tos](2)	0.92−1	1.8 ± 0.3	0^b	15 ± 3	2 ± 3	0
[C_4MIM][Tos](1)/CHO(2)	0.50−1	3.0 ± 0.2	60 ± 10	25 ± 2	3 ± 3	500 ± 100
CL(1)/[C_6MIM][NTf_2](2)^c	0.76−1			9.3 ± 0.3	−6.9 ± 0.3	

[a] Calculated with eq 3. [b] Assumed. [c] Ref 7.

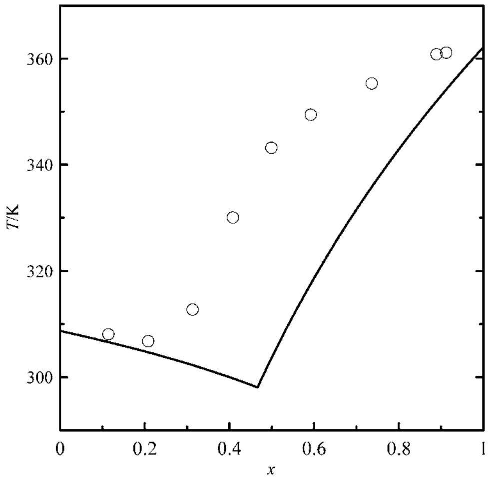

Figure 4. SLE for CHO + [C_{14}MIM][NTf_2]; *x*, mole fraction of CHO; ○, experimental points; —, ideal solubility curves.

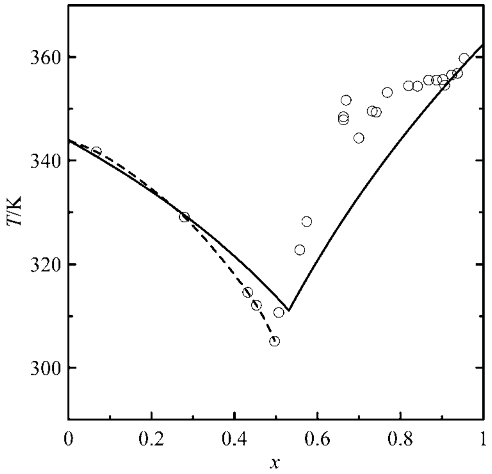

Figure 5. SLE for CHO + [C_4MIM][Tos]. *x*, mole fraction of CHO; ○, experimental points; —, ideal solubility curves, - - -, fitting curves (eq 1).

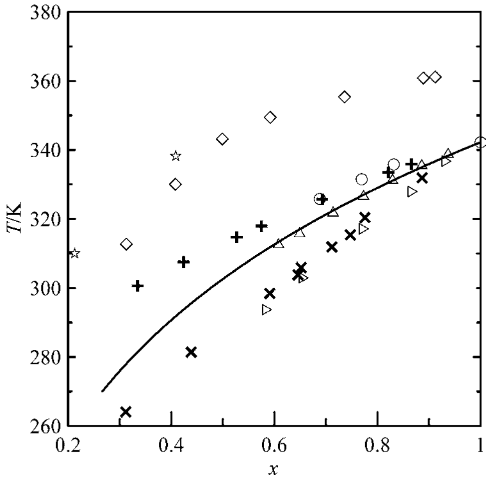

Figure 6. Solubility of CL and CHO in ILs; *x*, mole fraction of CL or CHO; ○, CL + [C_4MIM][BF_4]; +, CL + [C_4MIM][PF_6]; △, CL + [C_4MIM][Tos];[6] ×, CL + [C_6MIM][NTf_2];[7] right-pointing triangle, CL + [C_{14}MIM][NTf_2]; ◇, CHO + [C_{14}MIM][NTf_2]; ☆, CHO + [C_6MIM][NTf_2]; —, ideal solubility curve of CL.

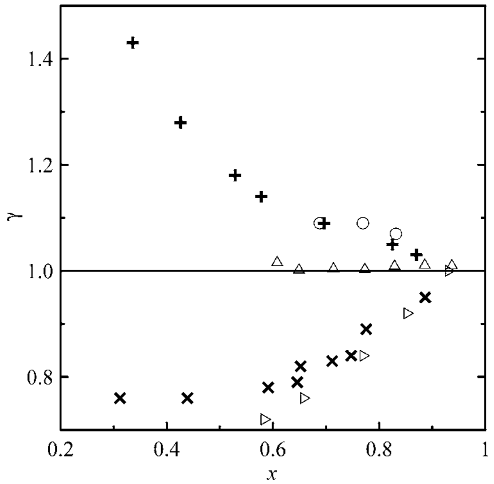

Figure 7. Activity coefficients of CL in the saturated CL + IL solutions; *x*, mole fraction of CL; ○, [C_4MIM][BF_4]; +, [C_4MIM][PF_6]; △, [C_4MIM][Tos]; ×, [C_6MIM][NTf_2];[7] right-pointing triangle, [C_{14}MIM][NTf_2]; —, $\gamma = 1$.

fractions of CL in the saturated solutions with [C_4MIM][PF_6] and [C_4MIM][BF_4] in the interval of x(CL) = 0.7 to 1 are close to each other, in spite of the fact that the anions of the ILs are significantly different: $[PF_6]^-$ is the hydrophobic anion, and $[BF_4]^-$ is the hydrophilic one. The solubility is lower than the ideal one in both cases. The solubility of CL in [C_4MIM][Tos] is close to the ideal one and exceeds it in the case of $[NTf_2]^-$ ILs. At the same time, the solubility of CL in [C_6MIM][NTf_2] is close to that in [C_{14}MIM][NTf_2]. So, one can conclude that the solubility of CL depends on the nature of the anion but not the alkyl chain of the cation. This conclusion agrees with ref 1. The activity coefficients of CL for its saturated solutions in ILs in the intervals of x(CL) where CL does not form intermolecular compounds with ILs are shown in Figure 7. At equal mole fractions, the activity coefficients of CL change as follows: [C_{14}MIM][NTf_2] ≈ [C_6MIM][NTf_2] < [C_4MIM][Tos] < [C_4MIM][PF_6] ≈ [C_4MIM][BF_4].

The solubility of CHO in ILs is lower than the ideal one, and in the case of [C_4MIM][BF_4] and [C_4MIM][PF_6] CHO and IL are mutually insoluble within the uncertainty of the used method. At equal mole fractions, the activity coefficients of CL change as follows: [C_4MIM][Tos] < [C_{14}MIM][NTf_2] ≈ [C_6MIM][NTf_2] < [C_4MIM][PF_6], [C_4MIM][BF_4]. The solubility of CL and CHO in ILs is different because of different parameters of melting (Table 2) and different affinities of CL and CHO toward ILs. One can see from Figure 6 that, for example, at 310 K solubility of CHO in [C_{14}MIM][NTf_2] is about 30 %, whereas the one of CL is more than 70 %.

To explain the difference in the activity coefficients of CL and CHO in the ILs we compared polarizabilities and dipole moments of CL and CHO. These parameters are often used to compare the affinity of solute and solvent.[15] The polarizabilities of CL and CHO molecules are almost equal: $\alpha(\text{CL}) = 10.9$ Å^3, $\alpha(\text{CHO}) = 11.3$ Å^3; but the dipole moments are different: $\mu(\text{CL}) = 4.0$ D, $\mu(\text{CHO}) = 0.9$ D. The dipole moments of the studied ILs are $\mu([C_4\text{mim}][BF_4]) = 11.8$ D, $\mu([C_4\text{mim}][PF_6]) = 13.6$ D, and $\mu([C_6\text{mim}][NTf_2]) = 16$ D. The lower dipole moment of the CHO molecule compared to that for CL may explain the difference of the activity coefficients in ILs which are the solvents of high polarity.

In spite of the fact that in ref 3 the use of [C_4mim][BF_4] and [C_4mim][PF_6] as reaction media for the Beckmann rearrangement was reported, we found that CHO and these ILs are mutually insoluble within the temperature interval of (290 to 370) K. The substantial difference in solubilities of CHO and CL in imidazolium-based ILs make limitations for their use as reaction media for a liquid-phase rearrangement of CHO into

CL. Preliminary tests with P_2O_5 that was used as a catalyst in ref 3 showed that this compound does not improve the solubility of CHO in ILs. The reaction can be carried out only in the four-component two-phase system CHO + IL + CL + catalyzer at the CHO−IL interface. In this case the product, CL, will pass into the IL phase.

Conclusion

Crystalline CHO is generally less soluble in imidazolium-based ILs with various anions than crystalline CL. The activity coefficients of CL in the saturated solutions take on the values more or less than 1, which mainly depends on the anion's nature. The activity coefficients of CHO are more than one in most cases and close to one in the saturated solution with $[C_4MIM][Tos]$. The difference of the solubilities makes serious problems for the use of these ILs as reaction media for the industrially important Beckmann rearrangement of CHO into CL.

The activity coefficients of CL in $[C_4MIM][PF_6]$ and $[C_4MIM][BF_4]$ decrease with temperature and mole fraction of IL. The activity coefficients of CL in $[C_6MIM][NTf_2]$ and $[C_{14}MIM][NTf_2]$ demonstrate the opposite temperature dependence.

Acknowledgment

The authors are grateful to Prof. A. Heintz from the University of Rostock (Germany) for the provided sample of $[C_4MIM][Tos]$ and Prof. Ya. S. Vygodskii from INEOS RAS (Moscow, Russia) for the sample of $[C_{14}MIM][NTf_2]$.

Literature Cited

(1) Wasserscheid, P.; Welton, T. *Ionic Liquids in Synthesis*; Wiley-VCH Verlag, GmbH&Co. KGaA: Weinheim, 2008.

(2) *Caprolactam production*; Ovchinnikov, V. I., Ed.; Khimiya: Moscow, 1977.

(3) Ren, R. X.; Zueva, L. D.; Ou, W. Formation of ε-caprolactam via Catalytic Beckmann Rearrangement Using P_2O_5 in Ionic Liquids. *Tetrahedron Lett.* **2001**, *42*, 8441–8443.

(4) Gui, J.; Deng, Y.; Hu, Zh.; Sun, Zh. A novel task-specific ionic liquid for Beckmann rearrangement: a simple and effective way for product separation. *Tetrahedron Lett.* **2004**, *45*, 2681–2683.

(5) Verevkin, S. P.; Emel'yanenko, V. N.; Toktonov, A. V.; Goodrich, P.; Hardacre, C. Thermochemistry of Ionic Liquid-Catalyzed Reactions: Theoretical and Experimental Study of the Beckmann Rearrangement−Kinetic or Thermodynamic Control. *Ind. Eng. Chem. Res.* **2009**, *48*, 9809–9816.

(6) Strechan, A. A.; Paulechka, Y. U.; Kabo, A. G.; Blokhin, A. V.; Kabo, G. J. 1-Butyl-3-methylimidazolium Tosylate Ionic Liquid: Heat Capacity, Thermal Stability, and Phase Equilibrium of Its Binary Mixtures with Water and Caprolactam. *J. Chem. Eng. Data* **2007**, *52*, 1791–1799.

(7) Shevelyova, M. P.; Zaitsau, D. H.; Paulechka, Y. U.; Blokhin, A. V.; Kabo, G. J. Solid-liquid equilibrium and activity coefficients for caprolactam + 1-hexyl-3-methylimidazolium bis(trifluoromethylsulfonyl)imide and cyclohexanone oxime + 1-hexyl-3-methylimidazolium bis(trifluoromethylsulfonyl)imide binaries. *J. Chem. Eng. Data* **2007**, *52*, 1360–1365.

(8) Kabo, G. J.; Blokhin, A. V.; Paulechka, Y. U.; Kabo, A. G.; Shymanovich, M. P. Thermodynamic Properties of 1-Butyl-3-methylimidazolium Hexafluorophosphate in the Condensed State. *J. Chem. Eng. Data* **2004**, *49*, 453–461.

(9) Paulechka, Y. U.; Kabo, A. G.; Blokhin, A. V.; Kabo, G. J.; Shevelyova, M. P. Heat Capacity of Ionic Liquids: Experimental Determination and Correlation with Molar Volume. *J. Chem. Eng. Data* **2010**, *55*, 2719–2724.

(10) Zaitsau, D. H.; Paulechka, Y. U.; Kabo, G. J.; Blokhin, A. V.; Emel'yanenko, V. N.; Verevkin, S. P.; Heintz, A. Thermodynamics of Cyclohexanone Oxime. *J. Chem. Eng. Data* **2008**, *53*, 694–703.

(11) Blokhin, A. V.; Kabo, G. J.; Paulechka, Y. U. Thermodynamic Properties of $[C_6mim][NTf_2]$ in the Condensed State. *J. Chem. Eng. Data* **2006**, *51*, 1377–1388.

(12) Walas, S. M. *Phase Equilibria in Chemical Engineering*; Butterworth Publishers: Boston, 1985.

(13) Granovsky, A. A. *Firefly*, version 7.1.G; MSU: Moscow, 2010.

(14) Schmidt, M. W.; Baldridge, K. K.; Boatz, J. A.; Elbert, S. T.; Gordon, M. S.; Jensen, J. H.; Koseki, S.; Matsunaga, N.; Nguyen, K. A.; Su, S.; Windus, T. L.; Dupuis, M.; Montgomery, J. A. General atomic and molecular electronic structure system. *J. Comput. Chem.* **1993**, *14*, 1347–1363.

(15) Hammett, L. P. *Physical Organic Chemistry*, 2nd ed.; McGraw Hill: New York, 1970.

Received for review May 13, 2010. Accepted December 27, 2010.

JE1005054